

The Illusion of Equivalency: Statistical Characterization of Quantization Effects in LLMs

Baha Rababah^{1,2}, Cuneyt Gurcan Akcora³, Carson K. Leung¹

¹ Department of Computer Science, University of Manitoba, Canada

² Applied Computer Education Department, Red River College Polytechnic, Canada

³ AI Initiative, University of Central Florida, USA

rababahb@myumanitoba.ca, carson.leung@umanitoba.ca, cuneyt.akcora@ucf.edu

Abstract

Post-training quantization is widely used to deploy large language models in resource-constrained settings, yet its evaluation relies almost exclusively on accuracy and perplexity. We show that these metrics fail to capture behavioral changes induced by quantization. We introduce correctness agreement, a decision-level metric that measures overlap in correct predictions between a base model and its quantized variants, independent of absolute accuracy. Across multiple models and quantization schemes from 8-bit to 2-bit, we find that behavioral divergence emerges under moderate quantization even when task performance appears preserved. To explain this effect, we analyze quantization as a structural operator on attention weights and quantify layer-wise distortions using statistical and distributional measures. Our results reveal non-linear breakpoints at low bit-widths and show that query and key projections are consistently more sensitive than value and output projections. These findings expose an illusion of equivalence between base and quantized models and motivate behavioral evaluation beyond conventional performance metrics.

1 Introduction

Recent advances in large language models (LLMs) have significantly improved text generation and reasoning capabilities [Ziyu *et al.*, 2023], but their growing size introduces substantial challenges for deployment in resource-constrained environments [Husom *et al.*, 2025]. Quantization, which reduces the numerical precision of model parameters and activations, has emerged as an effective approach to lowering memory footprint, accelerating inference, and reducing energy consumption [Jin *et al.*, 2024]. However, while quantization improves efficiency, it can also degrade performance and alter model behavior, particularly under aggressive low-bit precision settings [Dutta *et al.*, 2024].

The fundamental objective of quantization is to preserve the functional behavior of the original model while achieving computational efficiency. In practice, behavioral preservation extends beyond task-level accuracy to include factual knowledge, reasoning robustness, and consistent stylis-

tic and safety-related behaviors. These properties are especially vulnerable to quantization, as small numerical perturbations in model parameters may propagate non-linearly through deep architectures and lead to unexpected behavioral changes [Dutta *et al.*, 2024].

Despite this, existing quantization evaluations [Kurtic *et al.*, 2025; Li *et al.*, 2025; Jin *et al.*, 2024] rely on surface-level metrics such as accuracy, loss, and perplexity. While informative, these metrics do not fully capture whether quantization preserves behavioral consistency between the base model and its quantized variants. In particular, models with similar accuracy or perplexity may still differ substantially in their predictions on individual examples. To address this limitation, we introduce *correctness agreement*, a behavioral evaluation metric that measures the consistency of correct predictions between the original model and its quantized variants. Unlike aggregate performance metrics, our metric directly assesses whether quantization preserves decision-level behavior and provides a faithful signal of behavioral alignment under precision reduction.

Beyond behavioral evaluation, we provide a benchmark analysis of weight distribution shifts across a wide range of quantization levels (8-bit to 2-bit). This enables a fine-grained understanding of quantization as a continuous structural transformation and reveals how internal weight statistics and divergences evolve with lower precision. Our analysis exposes non-linear breakpoints where modest reductions in bit-width lead to disproportionate structural distortions, even when accuracy and perplexity appear stable. Examining multiple quantization bit-levels further allows us to isolate layer-wise and architecture-dependent sensitivities, identifying which components of LLMs are inherently robust and which are vulnerable to aggressive low-bit settings.

Our *key contributions* are as follows:

- We formalize post-training quantization as an operator family and study its joint impact on attention projection weights and decision behavior.
- We propose a statistical and divergence-based sensitivity analysis that quantifies layerwise structural drift using moments and distributional distances under quantization.
- We introduce *correctness agreement*, a decision-level metric that measures overlap in correct predictions be-

tween a base model and its quantized variants and complements accuracy and perplexity.

- To our knowledge, this work presents the first controlled sweep from 8-bit to 2-bit across legacy and K quantization that tracks block-level attention projection drift and links it empirically to decision behavior changes under post-training quantization.

2 Background and Related Work

Quantization reduces the numerical precision of neural network weights from floating point to lower bit representations in order to decrease model size, memory bandwidth usage, and inference cost on resource-constrained hardware [Xiao *et al.*, 2023]. Existing approaches fall into two categories: Quantization-Aware Training (QAT) and Post-Training Quantization (PTQ) [Jacob *et al.*, 2018]. QAT incorporates quantization during training and requires access to the training pipeline, making it expensive and impractical. In contrast, PTQ applies quantization directly to pretrained models without retraining, avoiding the cost of large-scale optimization. For this reason, PTQ is the dominant choice in practice and has been widely adopted for compressing LLMs while maintaining competitive accuracy [Detmers *et al.*, 2024; Kim *et al.*, 2024; Xiao *et al.*, 2023; Frantar *et al.*, 2022].

In this work, we use `llama.cpp` [Gerganov, 2024], the most widely adopted open source framework for post-training quantization. Its C/C++ implementation, broad hardware support, and extensive use in both research and production make it a de facto standard for practical LLMs quantization. We focus on the two quantization families implemented in `llama.cpp`: legacy quantization and K-quantization [Lee, 2025]. These methods jointly cover the full precision range from 8-bit to 2-bit and represent the most commonly used post-training quantization schemes in practice [Gerganov, 2024].

Legacy quantization methods (e.g. Q8_0, Q5_0, Q4_0) use block-wise uniform linear quantization with per-block scaling over fixed blocks of $k = 256$ weights. K-quantization methods (e.g. Q6_K, Q5_K, Q4_K, Q3_K, Q2_K) use a statistically informed block-based scheme that normalizes sub-blocks using estimates of the local mean and standard deviation. Implementation details are provided in Appendix A.1.

Table 1 summarizes evaluation dimensions across recent studies. Most prior work emphasizes aggregate task level measures such as accuracy and perplexity, which do not test whether the quantized model preserves the base model’s correct decisions on the same examples or connect internal weight distortions to decision behavior. Several studies focus on evaluating quantized LLMs that can be categorized into: (1) knowledge and capacity assessment, measuring correctness and reasoning ability [Hendrycks *et al.*, 2021; Shi *et al.*, 2024]; and (2) alignment evaluation, assessing adherence to human preferences and safety [Gehman *et al.*, 2020; Yin *et al.*, 2023]. Jin *et al.* [Jin *et al.*, 2024] proposed a structured evaluation framework spanning knowledge, alignment, and efficiency, showing that 4-bit quantization can maintain model performance. Another work by Kurtic *et al.* [Kurtic *et al.*,

Article	Stats	Div.	Bits	Layer	Behav.	Perf.
[Jin <i>et al.</i> , 2024]	✓	×	✓	×	×	✓
[Dutta <i>et al.</i> , 2024]	×	✓	×	×	✓	✓
[Gong <i>et al.</i> , 2024]	✓	×	×	✓	×	✓
[Kurtic <i>et al.</i> , 2025]	×	×	×	×	×	✓
[Husom <i>et al.</i> , 2025]	×	×	×	×	×	✓
[Güngör <i>et al.</i> , 2025]	×	×	×	×	×	✓
[Zhan <i>et al.</i> , 2025]	×	×	×	×	×	✓
[Li <i>et al.</i> , 2025]	×	×	×	×	×	✓
Our work	✓	✓	✓	✓	✓	✓

Table 1: Comparison of evaluation in **statistical analyses**, **divergence metrics**, evaluation across multiple quantization **bits**, **layer-wise sensitivity**, **behavioral evaluation**, and conventional **performance metrics**.

et al., 2025] analyzed FP8, INT8, and INT4 quantization across the LLaMA-3.1 family, illustrating that FP8 is effectively lossless, INT8 results in minimal accuracy reduction, and INT4 weight only quantization performs better than expected. However, these studies still focus only on task level performance, without systematically linking weight space changes to behavioral consistency or layer-wise vulnerabilities.

3 Methodology

Let \mathcal{V} be a vocabulary and let $\mathcal{X} \subseteq \mathcal{V}^*$ be the set of token sequences. A decoder-only transformer with N blocks and hidden width d is a parameterized conditional distribution $p_\theta(y | x)$, $x \in \mathcal{X}$, $y \in \mathcal{V}^*$, with parameters $\theta \in \mathbb{R}^P$ where P is the total number of trainable parameters.

For a prompt x and a target $y = (y_1, \dots, y_T)$, the model induces next-token probabilities $p_\theta(y | x) = \prod_{t=1}^T p_\theta(y_t | x, y_{<t})$. Let $\mathcal{D} = \{(x^{(m)}, y^{(m)})\}_{m=1}^M$ be an evaluation set, and let $\ell(\theta; x, y)$ be the token-level negative log-likelihood $\ell(\theta; x, y) := -\sum_{t=1}^{|y|} \log p_\theta(y_t | x, y_{<t})$. Perplexity on \mathcal{D} is defined as

$$\text{PPL}(\theta; \mathcal{D}) := \exp\left(\frac{1}{\sum_{m=1}^M |y^{(m)}|} \sum_{m=1}^M \ell(\theta; x^{(m)}, y^{(m)})\right).$$

Block and attention parameters. For block index $i \in [N] := \{1, \dots, N\}$, let the self-attention projection matrices be $W_i^Q, W_i^K, W_i^V, W_i^O \in \mathbb{R}^{d \times d}$. We denote the collection of attention matrices by $\mathcal{W}_\theta := \{W_i^L : i \in [N], L \in \{Q, K, V, O\}\}$. We view each $W \in \mathcal{W}_\theta$ as a vector in \mathbb{R}^{d^2} via $\text{vec}(W)$ when defining divergences.

Post-training quantization as an operator. We fix a finite set of quantization configurations \mathcal{C} , where each $c \in \mathcal{C}$ encodes a bit-width $b(c) \in \{2, 3, 4, 5, 6, 8\}$ and a scheme identifier (legacy or K-quantization). Let \mathcal{Q}_c be the quantizer and \mathcal{D}_c be the corresponding dequantizer. We model PTQ as an operator on parameters $T_c(\theta) := \mathcal{D}_c(\mathcal{Q}_c(\theta)) \in \mathbb{R}^P$. The quantized model induced by configuration c is $p_{T_c(\theta)}(y | x)$. Our core object of study is the joint effect of T_c on internal attention weights and on decision behavior over \mathcal{D} .

Structural deviation in attention weight space. For any matrix $W \in \mathcal{W}_\theta$, define its quantized-dequantized counter-

part as $\widehat{W}^{(c)} := W(T_c(\theta))$, and define the per-matrix deviation operator $\Delta_W^{(c)} := \widehat{W}^{(c)} - W$.

We quantify structural deviation using two families of functionals evaluated on model parameters. First, let $s(\cdot)$ be a statistical functional such as kurtosis, applied to the multiset of entries of a weight matrix. For each transformer block i , we define the block-level statistic for the base model as $\bar{s}_i(\theta) := \frac{1}{4} \sum_{L \in \{Q, K, V, O\}} s(W_i^L(\theta))$, and for a quantization configuration c as $\bar{s}_i^{(c)} := \bar{s}_i(T_c(\theta)) = \frac{1}{4} \sum_{L \in \{Q, K, V, O\}} s(\widehat{W}_i^{L, (c)})$. Aggregating across blocks gives the model-level statistics $\bar{s}(\theta) := \frac{1}{N} \sum_{i=1}^N \bar{s}_i(\theta)$, $\bar{s}^{(c)} := \frac{1}{N} \sum_{i=1}^N \bar{s}_i^{(c)}$. We define statistical drift under quantization configuration c as $\Delta \bar{s}^{(c)} := \bar{s}^{(c)} - \bar{s}(\theta)$. Second, let $d(\cdot, \cdot)$ be a divergence or similarity functional defined on tensors of equal shape. For each block i , we define the block-level divergence as $\bar{d}_i^{(c)} := \frac{1}{4} \sum_{L \in \{Q, K, V, O\}} d(\text{vec}(W_i^L(\theta)), \text{vec}(\widehat{W}_i^{L, (c)}))$, and aggregate across blocks to obtain $\bar{d}^{(c)} := \frac{1}{N} \sum_{i=1}^N \bar{d}_i^{(c)}$.

In our experiments, d includes cosine similarity, Euclidean distance, the Kolmogorov–Smirnov (KS) statistic, and Kullback–Leibler (KL) divergence, each computed from empirical histograms over weight entries.

Decision behavior and correctness agreement. We fix a benchmark task with a deterministic scoring functional $\text{score}(\cdot) : \mathcal{Y} \times \mathcal{Y} \rightarrow \{0, 1\}$, where $\text{score}(\hat{y}, y) = 1$ indicates a correct prediction under the task rubric. Let $g_\theta(x)$ denote the model’s predicted output for input x under a fixed scoring protocol. For multiple choice benchmarks, we score each candidate answer by the sum of token log probabilities under the model and select the argmax. This makes $g_\theta(x)$ deterministic given the tokenizer and scoring rule. For each example $m \in [M]$, define the base correctness label $z_m := \text{score}(g_\theta(x^{(m)}), y^{(m)}) \in \{0, 1\}$, and the quantized correctness label $z_m^{(c)} := \text{score}(g_{T_c(\theta)}(x^{(m)}), y^{(m)}) \in \{0, 1\}$. Accuracy is $\text{Acc}(\theta; \mathcal{D}) := \frac{1}{M} \sum_{m=1}^M z_m$, and similarly for $\text{Acc}(T_c(\theta); \mathcal{D})$.

Definition 1 (Correctness Agreement). Let z_m and $z_m^{(c)}$ be binary correctness labels (1 if correct, 0 otherwise) assigned to the predictions of the base and quantized models, respectively, on input $x^{(m)}$. The joint correctness between the two models is defined as

$$\text{CA}(c; \theta, \mathcal{D}) := \frac{1}{M} \sum_{m=1}^M \mathbb{1}[z_m = 1 \wedge z_m^{(c)} = 1],$$

where M is the number of evaluation examples in \mathcal{D} .

The agreement metric also satisfies the bound: $0 \leq \text{CA}(c; \theta, \mathcal{D}) \leq \min\{\text{Acc}(\theta; \mathcal{D}), \text{Acc}(T_c(\theta); \mathcal{D})\} \leq 1$. This follows since $\mathbb{1}[z_m = 1 \wedge z_m^{(c)} = 1] \leq z_m$ and $\leq z_m^{(c)}$ for every m . Hence, CA is always in $[0, 1]$, but its scale is tied to the base and quantized model accuracies.

Although downstream tasks may involve multiclass prediction, the correctness is computed on binary correctness

indicators (correct vs. incorrect) for each example. Unlike standard accuracy, this metric captures the overlap in correct predictions between the base and quantized models, and disregards cases where both models are jointly incorrect.

Problem statement. Given a pretrained model p_θ and a family of post-training quantization operators $\{T_c\}_{c \in \mathcal{C}}$, we aim to analyze how quantization affects model behavior. We link structural deviation in attention projection weights, quantified via statistics and divergence metrics, to behavioral drift on downstream tasks, measured through accuracy and correctness agreement. Using evaluation sets \mathcal{D}_{pp1} (perplexity needs raw text with token-level likelihood) and $\mathcal{D}_{\text{bench}}$ (using a task-specific scoring function), we track how consistency with the base model degrades as precision decreases.

Our analysis proceeds in two stages. First, we evaluate changes in internal weight distributions across quantization levels (8-bit to 2-bit) using statistical and distributional metrics. Second, we relate these changes to model behavior through perplexity, accuracy, and correctness agreement. This approach identifies how internal perturbations correlate with behavioral inconsistency and reveals which components are most sensitive to low-bit quantization.

3.1 Quantification of Statistical Changes

We compute summary statistics on the K , Q , V , and O projection weights in every transformer block for the base model and for quantized models after dequantization, which reconstructs approximate floating-point weights. We focus on four statistics: mean, standard deviation, skewness, and kurtosis [Virtanen *et al.*, 2020].

For each attention projection $L \in K, Q, V, O$ across all N blocks, we perform two analyses. First, we aggregate statistics across the four projections within each block to obtain a block-level view of structural change. Second, we compare statistics per projection across quantization levels to expose layer-specific sensitivity. Mean captures quantization-induced bias, standard deviation captures scale distortion, skewness captures asymmetric perturbations, and kurtosis captures the degradation of heavy tails that encode rare but influential weights.

Average Statistics Across All Attention Layers. The average statistics across all attention layers are calculated according to Eq. (1) which defines the average layer-wise metric used in our analysis. For each transformer block i , the statistical metric is computed independently for the four self-attention projection matrices: query (Q_i), key (K_i), value (V_i), and output (O_i). These four values are averaged to obtain a single attention-level score per block, and the resulting scores are then averaged across all blocks. This produces a summary of quantization effects on the attention weight space. After computing this aggregated statistic for the base model and its quantized variants, we compare the resulting values to measure how quantization alters the attention weight structure compared to the original model.

$$\bar{s}(\theta) := \frac{1}{N} \sum_{i=1}^N \left(\frac{1}{|L|} \sum_{L \in \{Q, K, V, O\}} s(W_i^L(\theta)) \right). \quad (1)$$

Individual Statistics Comparison. To isolate the effect of quantization on each attention projection type, we compute statistics separately for each layer component $L \in \{Q, K, V, O\}$. For a given statistical functional $s(\cdot)$, we evaluate $s(W_i^L)$ independently across all N blocks and average the results. This gives a layer-specific summary of structural drift, capturing how quantization affects each projection type throughout the model. For example, computing $s(W_i^Q)$ for all i quantifies distortion in the query projections.

$$\bar{s}_L := \frac{1}{N} \sum_{i=1}^N s(W_i^L). \quad (2)$$

3.2 Quantification of Distributional Divergence

We complement the statistical analysis with divergence-based measures to quantify structural deviation between the base model and its quantized variants. For each transformer block i , we compute a divergence metric between corresponding weight matrices W_i^L and $\widehat{W}_i^{L,(c)}$ for each projection type $L \in \{Q, K, V, O\}$. The resulting values are used to compute both block-level and layer-specific measures of structural drift.

We consider four divergence metrics: (1) *Kolmogorov–Smirnov statistic*, which measures the maximum difference between cumulative distributions; (2) *Euclidean distance*, capturing magnitude differences between weight vectors; (3) *Cosine similarity*, measuring angular alignment; and (4) *Kullback–Leibler divergence*, which quantifies divergence between empirical histograms of weight values [Virtanen *et al.*, 2020]. These metrics capture complementary aspects of structural change, spanning orientation in parameter space, scale distortion, and redistribution of mass across weight values.

Average Divergence Across All Attention Layers. We use Eq. (1) to compute the average divergence across K , Q , V , and O projections in each block. These per-block averages are then aggregated across all N blocks to yield a model-level summary. This provides a coarse-grained view of structural deviation under quantization.

Individual Divergence Comparison. To examine sensitivity by projection type, we compute divergence metrics separately for each $L \in \{Q, K, V, O\}$ using Eq. (2). This isolates which attention components are most affected by low-bit quantization and reveals asymmetric patterns across Q , K , V , and O .

3.3 Sensitivity and Behavioral Analysis Across Quantization Levels

Layer-wise Sensitivity Analysis. To identify which attention components are most affected by quantization, we examine statistical and divergence metrics independently for each projection type (Q , K , V , O). Layers exhibiting the largest deviations from the base model are considered more sensitive. This analysis reveals non-uniform sensitivity patterns across attention components and informs selective or mixed-precision quantization strategies.

Quantization Level Comparison. We compare models across multiple quantization levels to study how decreasing precision affects both weight-space structure and behavioral consistency. By tracking trends in statistics, divergence, perplexity, accuracy, and correctness agreement, we identify critical precision thresholds at which quantization begins to degrade performance or induce behavioral drift.

Behavioral Evaluation. We evaluate the base model and its quantized variants using standard task-level and behavioral metrics to connect structural changes in weight space to observable behavior. Specifically, we measure perplexity and accuracy to assess aggregate performance, and correctness agreement to quantify decision-level consistency. Joint analysis of these behavioral metrics with statistical and divergence-based measures reveals regimes where surface-level performance remains stable despite increasing structural distortion, as well as thresholds where such distortions translate into behavioral inconsistency.

4 Experimental Results

We quantize the following four models: Llama-3.2-3B, Vicuna-7B-v1.5, Mistral-7B-v0.1, and Llama-3.1-8B into legacy quantization methods (Q8_0, Q5_0, Q4_0) and K-quantization methods (Q6_K, Q5_K, Q4_K, Q3_K, Q2_K) using llama.cpp [Gerganov, 2024]. We extract the layers’ weights of the base models and its quantized variants after dequantization.

Datasets. We evaluate quantized models using both language modeling corpora and downstream benchmark tasks. For perplexity evaluation, we use WikiText-2 [Merity *et al.*, 2017] and C4 [Raffel *et al.*, 2020]. To assess task-level performance and behavioral consistency, we use zero-shot benchmarks including HellaSwag [Zellers *et al.*, 2019], Winogrande [Sakaguchi *et al.*, 2019], and ARC (AI2 Reasoning Challenge) [Clark *et al.*, 2018]. These datasets cover a range of commonsense reasoning and structured problem-solving tasks.

We evaluate the models on eight NVIDIA Tesla V100-SXM2 GPUs (32GB HBM2 each). Our Python implementation is included in the submission.

4.1 Statistical Changes in Attention Layers

For each transformer block i , we compute a block-level statistic by averaging $s(W_i^Q)$, $s(W_i^K)$, $s(W_i^V)$, and $s(W_i^O)$, and then aggregate these values across all N blocks as defined in Eq. (1). This yields a global view of how attention-weight distributions evolve under different quantization levels. The aggregated results are shown in Fig. 1.

Figure 1 shows that higher-bit quantization schemes (8 to 5 bits) largely preserve the statistical properties of attention weights, with near-zero mean, low skewness, stable kurtosis, and baseline-level standard deviation across models. In contrast, aggressive low-bit quantization (4 to 2 bits), particularly Q3_K and Q2_K, introduces pronounced distortions, including increased skewness and variance, reduced kurtosis, and systematic mean shifts. These effects are model-dependent, with smaller models such as Llama-3.2-3B exhibiting larger

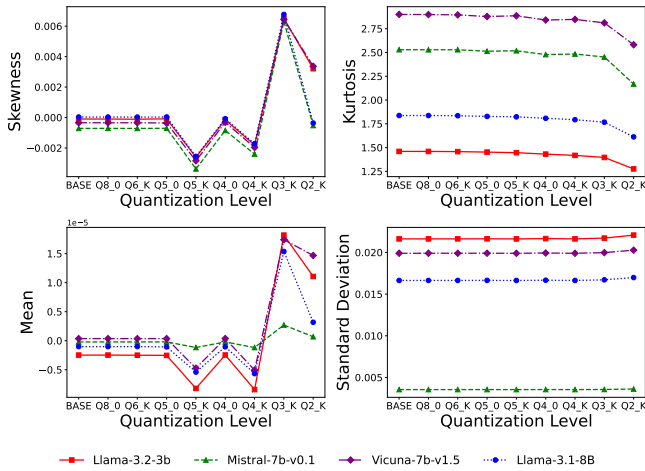


Figure 1: Aggregated statistical metrics across legacy and K-quantization methods.

deviations. Notably, Q5_0 closely matches the base model across all statistical metrics, indicating strong preservation of distributional structure at moderate compression.

Individual Statistic Comparison. To examine layer-specific effects, we compute statistics independently for each attention projection type (K , Q , V , O) by averaging $s(W_i^L)$ across all N blocks, as defined in Eq. (2). This analysis reveals how quantization impacts individual attention components beyond the aggregated view.

For legacy quantization schemes (Q8_0, Q5_0, Q4_0), layer-wise statistics remain nearly identical to the base model across all metrics; legacy quantization has minimal structural impact. Representative plots are provided in Appendix 4.1.

In contrast, K-quantization results in Fig. 2 for skew and Fig. 3 for kurtosis expose clear layer-dependent sensitivity as precision decreases. Moderate K-quantization levels (Q6_K–Q4_K) preserve attention-layer statistics across Q , K , V , and O , maintaining stable distribution shape, tail behavior, and variance. However, aggressive low-bit settings (Q3_K and Q2_K) lead to substantial distortions, particularly in the Q and K projections, where skewness becomes volatile, kurtosis collapses, and mean and variance deviate sharply from the base model. The V and O projections remain comparatively stable under the same conditions, except for the Q2_K.

This analysis shows that legacy quantization introduces negligible statistical distortion, whereas K-quantization induces non-uniform, layer-dependent effects at low bit-widths. In particular, the Q and K projections consistently emerge as the most sensitive to aggressive compression, a pattern that recurs across all evaluated models.

4.2 Distributional Divergence in Attention Layers

We complement the statistical analysis with distributional divergence measures to quantify how quantization alters the structure of attention weight distributions. For each transformer block i , we compute divergence metrics between the base and quantized weight matrices for each attention projection $L \in \{Q, K, V, O\}$, and aggregate these values across blocks as defined in Section 3.2.

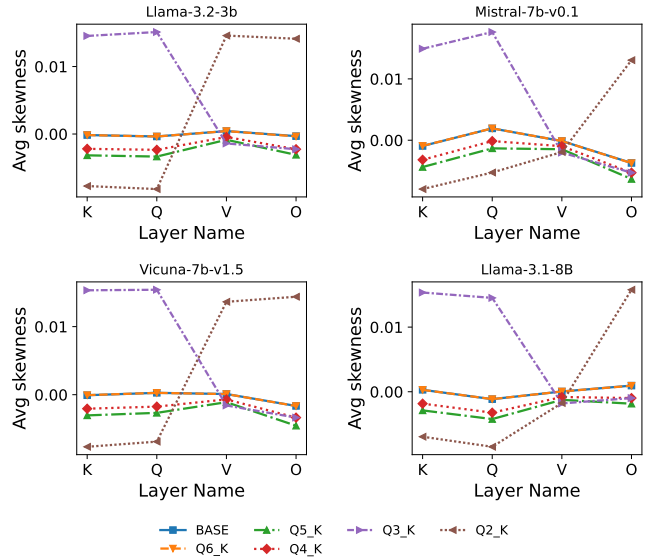


Figure 2: Average skewness across attention layers under K-quantization.

Aggregated Divergence Across Quantization Levels.

Figure 4 shows the aggregated divergence trends across quantization levels for all models. Cosine similarity remains high at moderate bit-widths and degrades gradually as precision decreases. In contrast, KL divergence and the KS statistic exhibit sharp increases at lower-bit quantization levels, indicating substantial redistribution of weight values. Euclidean distance varies comparatively little across quantization settings and is less sensitive to precision reduction.

Layer-Specific Divergence. To examine component-wise effects, we compute divergence metrics separately for each attention projection. Figure 5 shows the per-layer KL divergence under K-quantization. Divergence increases are not uniform across attention components: the Q and K projections consistently exhibit larger distributional shifts as bit-width decreases, while the V and O projections remain comparatively stable across the same quantization levels. Additional per-layer divergence plots, including legacy quantization results and KS statistics, are provided in Appendix 3.2.

4.3 Performance Evaluations

We evaluate quantized models using both language modeling and downstream benchmark tasks to assess how quantization affects surface-level performance and decision-level behav-

Quant	Llama-3.2-3B	Vicuna-7B	Mistral-7B	Llama-3.1-8B
Base	2.300 ± 0.056	2.462 ± 0.013	2.333 ± 0.021	2.167±0.015
Q8.0	2.303 ± 0.006	<u>2.450 ± 0.010</u>	2.317 ± 0.035	2.203±0.023
Q6.K	2.250 ± 0.010	2.473 ± 0.059	2.330 ± 0.010	2.190±0.000
Q5.0	2.170 ± 0.010	2.760 ± 0.046	2.380 ± 0.010	2.187±0.006
Q5.K	2.223 ± 0.023	2.459 ± 0.075	<u>2.290 ± 0.026</u>	2.167±0.006
Q4.0	2.313 ± 0.029	2.853 ± 0.034	2.440 ± 0.026	<u>2.030±0.017</u>
Q4.K	2.307 ± 0.015	2.502 ± 0.036	2.330 ± 0.017	2.170±0.010
Q3.K	<u>1.967 ± 0.006</u>	2.361 ± 0.023	2.333 ± 0.025	2.033±0.023
Q2.K	1.857 ± 0.012	2.770 ± 0.010	2.120 ± 0.020	1.687±0.006

Table 2: Perplexity (\downarrow) on WikiText2

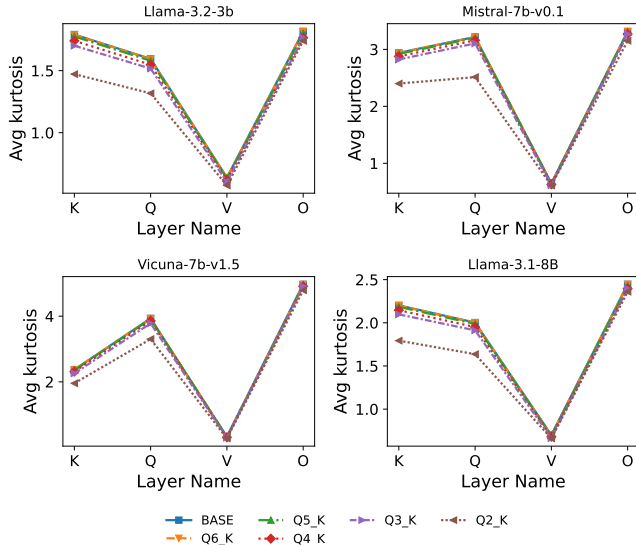


Figure 3: Average kurtosis across attention layers under K-quantization.

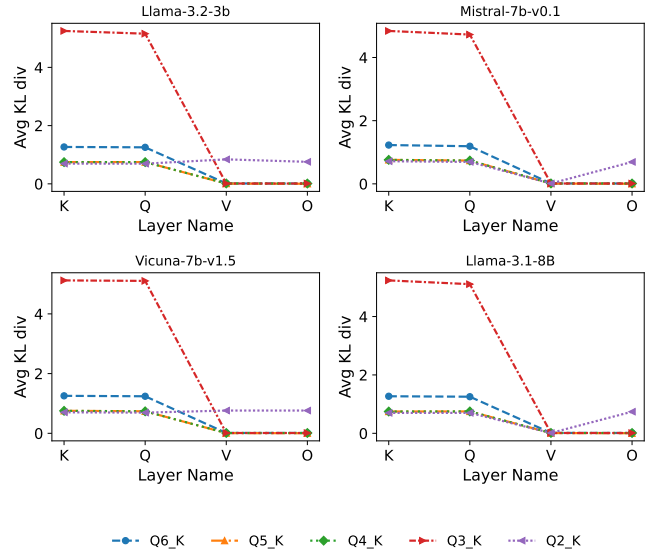


Figure 5: Average KL K-Quantization.

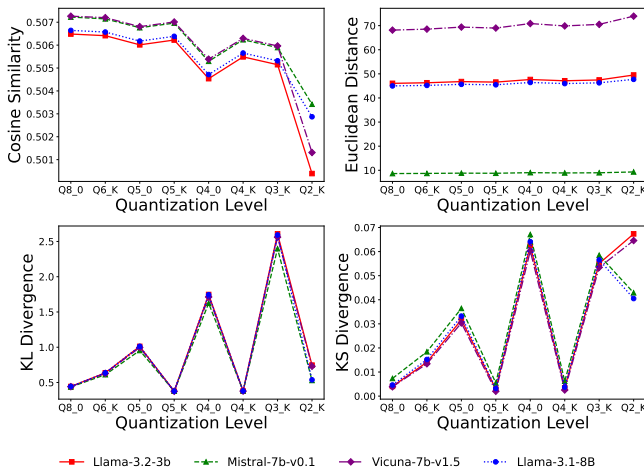


Figure 4: Comparison of aggregated similarity and divergence metrics across quantization methods.

ior. Full experimental details and additional results are provided in Appendix A.6.

Perplexity. We measure language modeling perplexity on WikiText 2 [Merity *et al.*, 2017] and C4 [Raffel *et al.*, 2020]. Perplexity does not change monotonically with bit width and the effect depends on the base model and dataset. Tables 2 and 3 show that several mid-range quantization configurations preserve perplexity close to the base model for Llama 3.2 3B and Llama 3.1 8B, while Vicuna 7B shows larger increases on C4 under multiple quantization settings. In particular, K quantization configurations in the mid range from Q6_K to Q5_0 avoid the sharp degradation observed under more aggressive compression. Lower bit schemes such as Q3_K can yield lower perplexity in some cases, but this behavior is model-dependent and dataset-dependent and does not generalize. This instability shows that perplexity is not a reliable proxy for preserved decisions under quantization.

Downstream Accuracy. We evaluate zero-shot task performance on HellaSwag [Zellers *et al.*, 2019], Winogrande [Sakaguchi *et al.*, 2019], and ARC [Clark *et al.*, 2018]. As shown in Table 4, accuracy generally decreases as quantization becomes more aggressive. Larger models exhibit greater robustness, while smaller models experience more pronounced degradation at low bit-widths. Mid-range quantization levels retain accuracy reasonably close to the base model, whereas Q3_K and Q2_K consistently underperform.

Correctness Agreement. Table 4 reports correctness agreement, the fraction of examples where both the base and quantized models are correct. Correctness agreement is consistently below accuracy and decreases as precision decreases, indicating that fewer base model correct decisions remain correct after quantization, even when aggregate performance remains close to the base model.

Overall, perplexity and accuracy can remain stable under moderate quantization, while decision-level agreement with the base model drops sharply. This shows that conventional metrics miss behavioral drift and must be complemented with behavioral evaluation.

5 Discussion

This section synthesizes the experimental findings to assess the impact of quantization on language model behavior, sta-

Quant	Llama-3.2-3B	Vicuna-7B	Mistral-7B	Llama-3.1-8B
Base	8.357 ± 0.230	4.070 ± 0.041	4.070 ± 0.041	7.400 ± 0.128
Q8_0	8.253 ± 0.165	6.038 ± 0.157	4.067 ± 0.046	7.600 ± 0.035
Q6_K	8.120 ± 0.085	6.154 ± 0.111	4.007 ± 0.006	<u>7.293 ± 0.061</u>
Q5_0	8.203 ± 0.114	6.397 ± 0.108	4.073 ± 0.035	7.467 ± 0.051
Q5_K	<u>8.057 ± 0.049</u>	6.063 ± 0.217	4.040 ± 0.072	7.147 ± 0.176
Q4_0	8.763 ± 0.116	6.394 ± 0.128	4.152 ± 0.018	7.293 ± 0.144
Q4_K	8.353 ± 0.195	6.183 ± 0.009	4.060 ± 0.052	7.500 ± 0.173
Q3_K	7.823 ± 0.075	<u>5.977 ± 0.083</u>	<u>4.027 ± 0.025</u>	8.037 ± 0.151
Q2_K	8.730 ± 0.104	6.556 ± 0.096	4.040 ± 0.030	8.243 ± 0.266

Table 3: Perplexity (\downarrow) on C4

Quant	Llama 3.2 3B		Vicuna 7B		Mistral 7B		Llama 3.1 8B	
	Accuracy	CA	Accuracy	CA	Accuracy	CA	Accuracy	CA
Base	55.5±15.02	–	58.9±14.68	–	61.6±16.70	–	60.9±17.83	–
Q8_0	53.4±9.04	41.4±15.8	55.6±9.75	46.7±15.56	56.9±11.76	48.2±17.89	55.0±8.17	45.6±14.21
Q6_K	52.9±8.50	<u>41.1±14.73</u>	56.1±9.69	46.1±16.59	56.5±11.38	48.1±17.58	54.8±8.28	45.7±14.56
Q5_0	52.6±8.46	41.0±14.05	55.3±9.78	45.7±16.45	56.6±12.33	<u>48.3±18.03</u>	54.1±8.44	45.1±14.45
Q5_K	52.8±9.25	41.0±15.25	56.1±9.00	46.3±16.19	56.4±10.97	47.9±17.55	55.0±8.96	45.9±14.98
Q4_0	52.4±6.81	40.8±12.60	56.0±10.44	45.2±17.77	<u>56.9±11.90</u>	48.5±17.71	54.5±8.88	45.3±14.62
Q4_K	52.1±7.51	40.9±13.73	56.3±9.68	46.3±16.82	56.0±11.43	47.7±17.71	55.1±8.88	45.8±14.87
Q3_K	51.5±8.40	39.9±14.08	<u>56.8±11.11</u>	46.9±17.07	55.5±11.90	47.7±17.83	<u>55.7±9.87</u>	46.0±15.76
Q2_K	48.7±8.43	38.5±12.11	<u>53.7±7.56</u>	42.9±14.80	55.5±10.59	47.3±15.74	<u>52.4±9.37</u>	44.1±13.15

Table 4: Macro average accuracy and correctness agreement CA across HellaSwag, Winogrande, and ARC. Base uses identity so CA equals accuracy.

tistical stability, and structural fidelity.

Statistical and Divergence Analysis Reveals Critical Low-Bit Structural Changes. Across all models, weight statistics and divergences remain stable under high and moderate bit quantization (Q8_0, Q6_K, Q5_0, Q5_K), with near-zero skewness and mean, consistent kurtosis across layers, and minimal drift in standard deviation. The structural perturbations start at Q4_K and Q4_0, while the most extreme distortions occur at Q3_K and Q2_K, where skewness spikes, mean shifts upward, and kurtosis collapses, indicating noisier distributions. Cosine similarity drops and KL divergence rises at low-bit levels, showing that weight vectors increasingly deviate from their base model. **Thus, these metrics reveal that performance degradation aligns with pronounced structural deviations in attention weight statistics and geometry.**

K and Q Layers are Most Sensitive to Quantization. The analyses reveal that the **K** and **Q** layers are sensitive to quantization. Under Q3_K and Q2_K, these layers exhibit the largest spikes in skewness, the greatest shifts in mean, and the steepest drops in kurtosis. In contrast, the **V** layer preserves its low-kurtosis profile even under moderate compression, and the **O** layer, despite having the highest kurtosis, remains relatively stable until the lowest quantization levels. Divergence metrics reinforce this pattern: cosine similarity and KL divergence deviate most strongly for **K** and **Q**. This indicates that future quantization methods may benefit from adaptive strategies that allocate higher precision to **K** and **Q** while compressing **V** and **O** more aggressively.

Quantization does not Preserve Base Model Behavior. Quantization changes decision behavior relative to the base model across all models and bit configurations. Even at higher precision settings, correctness agreement remains below the base model accuracy ceiling, indicating that many base model correct decisions do not remain correct after quantization. This gap widens in low bit regimes, with the largest drops under Q3_K and Q2_K.

Quantization Reveals Disconnect Between Perplexity and Output Consistency. Although configurations such as Q3_K and Q5_K achieve low perplexity, particularly for Llama-3.2-3B and Vicuna-7B. This does not translate to agreement with the Base model, revealing a disconnect between task performance and output-level consistency. More aggressive quantization (Q3_K and Q2_K) further am-

plifies behavioral drift, producing the lowest agreement and confirming that reduced bit-width increases divergence from the Base model’s predictions. Overall, these results demonstrate that quantized variants do not reliably reproduce base-model behavior, even when accuracy or perplexity appears preserved.

6 Conclusion

We have presented a systematic analysis of how post-training quantization affects both the internal structure and behavioral consistency of LLMs. By jointly examining attention-weight statistics, divergence measures, and agreement at the output level, we have shown that quantization causes structural distortions not captured by accuracy and perplexity. Even moderate quantization significantly reduces behavioral agreement with the base model, whereas low-bit schemes cause critical statistical and geometric disruption. Across all models and metrics, we have identified Q4_K as the upper bound of safe quantization, Q3_K as the start of degradation, and Q2_K as a breakdown regime. We have further shown that the **K** and **Q** layers are the most sensitive to quantization, motivating future structure-aware precision allocation strategies.

References

- [Clark *et al.*, 2018] Peter Clark, Isaac Cowhey, Oren Etzioni, Tushar Khot, Ashish Sabharwal, Carissa Schoenick, and Oyvind Tafjord. Think you have solved question answering? try arc, the ai2 reasoning challenge. *arXiv preprint arXiv:1803.05457*, 2018.
- [Dettmers *et al.*, 2024] Tim Dettmers, Ruslan Svirschevski, Vage Egiazarian, Denis Kuznedelev, Elias Frantar, Saleh Ashkboos, Alexander Borzunov, Torsten Hoefer, and Dan Alistarh. Spqr: A sparse-quantized representation for near-lossless LLM weight compression. In *The Twelfth International Conference on Learning Representations, ICLR 2024, Vienna, Austria, May 7-11, 2024*. OpenReview.net, 2024.
- [Dutta *et al.*, 2024] Abhinav Dutta, Sanjeev Krishnan, Nipun Kwatra, and Ramachandran Ramjee. Accuracy is not all you need. In Amir Globersons, Lester Mackey, Danielle Belgrave, Angela Fan, Ulrich Paquet, Jakub M. Tomczak,

- and Cheng Zhang, editors, *Advances in Neural Information Processing Systems 38: Annual Conference on Neural Information Processing Systems 2024, NeurIPS 2024, Vancouver, BC, Canada, December 10 - 15, 2024*, 2024.
- [Frantar *et al.*, 2022] Elias Frantar, Saleh Ashkboos, Torsten Hoefler, and Dan Alistarh. GPTQ: accurate post-training quantization for generative pre-trained transformers. *CoRR*, abs/2210.17323, 2022.
- [Gehman *et al.*, 2020] Samuel Gehman, Suchin Gururangan, Maarten Sap, Yejin Choi, and Noah A. Smith. Realtotoxicityprompts: Evaluating neural toxic degeneration in language models. In Trevor Cohn, Yulan He, and Yang Liu, editors, *Findings of the Association for Computational Linguistics: EMNLP 2020, Online Event, 16-20 November 2020*, volume EMNLP 2020 of *Findings of ACL*, pages 3356–3369. Association for Computational Linguistics, 2020.
- [Gerganov, 2024] Georgi Gerganov. Llama.cpp. Online, 2024. Accessed: Nov. 8, 2025.
- [Gong *et al.*, 2024] Ruihao Gong, Yang Yong, Shiqiao Gu, Yushi Huang, Chengtao Lv, Yunchen Zhang, Dacheng Tao, and Xianglong Liu. LLMC: benchmarking large language model quantization with a versatile compression toolkit. In Franck Dernoncourt, Daniel Preotiuc-Pietro, and Anastasia Shimorina, editors, *Proceedings of the 2024 Conference on Empirical Methods in Natural Language Processing: EMNLP 2024 - Industry Track, Miami, Florida, USA, November 12-16, 2024*, pages 132–152. Association for Computational Linguistics, 2024.
- [Güngör *et al.*, 2025] Onat Güngör, Roshan Sood, Harold Wang, and Tajana Rosing. AQUA-LLM: evaluating accuracy, quantization, and adversarial robustness trade-offs in llms for cybersecurity question answering. *CoRR*, abs/2509.13514, 2025.
- [Hendrycks *et al.*, 2021] Dan Hendrycks, Collin Burns, Steven Basart, Andy Zou, Mantas Mazeika, Dawn Song, and Jacob Steinhardt. Measuring massive multitask language understanding. In *9th International Conference on Learning Representations, ICLR 2021, Virtual Event, Austria, May 3-7, 2021*. OpenReview.net, 2021.
- [Husom *et al.*, 2025] Erik Johannes Husom, Arda Goknil, Merve Astekin, Lwin Khin Shar, Andre Käsen, Sagar Sen, Benedikt Andreas Mithassel, and Ahmet Soylu. Sustainable LLM inference for edge AI: evaluating quantized llms for energy efficiency, output accuracy, and inference latency. *CoRR*, abs/2504.03360, 2025.
- [Jacob *et al.*, 2018] Benoit Jacob, Skirmantas Kligys, Bo Chen, Menglong Zhu, Matthew Tang, Andrew G. Howard, Hartwig Adam, and Dmitry Kalenichenko. Quantization and training of neural networks for efficient integer-arithmetic-only inference. In *2018 IEEE Conference on Computer Vision and Pattern Recognition, CVPR 2018, Salt Lake City, UT, USA, June 18-22, 2018*, pages 2704–2713. Computer Vision Foundation / IEEE Computer Society, 2018.
- [Jin *et al.*, 2024] Renren Jin, Jiangcun Du, Wuwei Huang, Wei Liu, Jian Luan, Bin Wang, and Deyi Xiong. A comprehensive evaluation of quantization strategies for large language models. In Lun-Wei Ku, Andre Martins, and Vivek Srikumar, editors, *Findings of the Association for Computational Linguistics, ACL 2024, Bangkok, Thailand and virtual meeting, August 11-16, 2024*, pages 12186–12215. Association for Computational Linguistics, 2024.
- [Kim *et al.*, 2024] Sehoon Kim, Coleman Hooper, Amir Gholami, Zhen Dong, Xiuyu Li, Sheng Shen, Michael W. Mahoney, and Kurt Keutzer. Squeezellm: Dense-and-sparse quantization. In *Forty-first International Conference on Machine Learning, ICML 2024, Vienna, Austria, July 21-27, 2024*. OpenReview.net, 2024.
- [Kurtic *et al.*, 2025] Eldar Kurtic, Alexandre Noll Marques, Shubhra Pandit, Mark Kurtz, and Dan Alistarh. "give me BF16 or give me death"? accuracy-performance trade-offs in LLM quantization. In Wanxiang Che, Joyce Nabende, Ekaterina Shutova, and Mohammad Taher Pilehvar, editors, *Proceedings of the 63rd Annual Meeting of the Association for Computational Linguistics (Volume 1: Long Papers), ACL 2025, Vienna, Austria, July 27 - August 1, 2025*, pages 26872–26886. Association for Computational Linguistics, 2025.
- [Lee, 2025] Jaesik Lee. Quantization-based jailbreaking vulnerability analysis: A study on performance and safety of the llama3-8b-instruct model. *IEEE Access*, 13:136524–136535, 2025.
- [Li *et al.*, 2025] Zhen Li, Yupeng Su, Runming Yang, Zhongwei Xie, Ngai Wong, and Hongxia Yang. Quantization meets reasoning: Exploring LLM low-bit quantization degradation for mathematical reasoning. *CoRR*, abs/2501.03035, 2025.
- [Merity *et al.*, 2017] Stephen Merity, Caiming Xiong, James Bradbury, and Richard Socher. Pointer sentinel mixture models. In *5th International Conference on Learning Representations, ICLR 2017, Toulon, France, April 24-26, 2017, Conference Track Proceedings*. OpenReview.net, 2017.
- [Raffel *et al.*, 2020] Colin Raffel, Noam Shazeer, Adam Roberts, Katherine Lee, Sharan Narang, Michael Matena, Yanqi Zhou, Wei Li, and Peter J. Liu. Exploring the limits of transfer learning with a unified text-to-text transformer. *J. Mach. Learn. Res.*, 21:140:1–140:67, 2020.
- [Sakaguchi *et al.*, 2019] Keisuke Sakaguchi, Ronan Le Bras, Chandra Bhagavatula, and Yejin Choi. Winogrande: An adversarial winograd schema challenge at scale. *arXiv preprint arXiv:1907.10641*, 2019.
- [Shi *et al.*, 2024] Dan Shi, Chaobin You, Jiantao Huang, Taihao Li, and Deyi Xiong. CORECODE: A common sense annotated dialogue dataset with benchmark tasks for chinese large language models. In Michael J. Wooldridge, Jennifer G. Dy, and Sriraam Natarajan, editors, *Thirty-Eighth AAAI Conference on Artificial Intelligence, AAAI 2024, Thirty-Sixth Conference on Innovative Applications*

of Artificial Intelligence, IAAI 2024, Fourteenth Symposium on Educational Advances in Artificial Intelligence, EAAI 2014, February 20-27, 2024, Vancouver, Canada, pages 18952–18960. AAAI Press, 2024.

[Virtanen *et al.*, 2020] Pauli Virtanen, Ralf Gommers, Travis E. Oliphant, Matt Haberland, Tyler Reddy, David Cournapeau, Evgeni Burovski, Pearu Peterson, Warren Weckesser, Jonathan Bright, Stéfan J. van der Walt, Matthew Brett, Joshua Wilson, K. Jarrod Millman, Nikolay Mayorov, Andrew R. J. Nelson, Eric Jones, Robert Kern, Eric Larson, CJ Carey, İlhan Polat, Yu Feng, Eric W. Moore, Jake VanderPlas, Denis Laxalde, Josef Perktold, Robert Cimrman, Ian Henriksen, E. A. Quintero, Charles R. Harris, Anne M. Archibald, Antônio H. Ribeiro, Fabian Pedregosa, and Paul van Mulbregt. Scipy 1.0: Fundamental algorithms for scientific computing in python. *Nature Methods*, 17:261–272, 2020.

[Xiao *et al.*, 2023] Guangxuan Xiao, Ji Lin, Mickaël Seznec, Hao Wu, Julien Demouth, and Song Han. Smoothquant: Accurate and efficient post-training quantization for large language models. In Andreas Krause, Emma Brunskill, Kyunghyun Cho, Barbara Engelhardt, Sivan Sabato, and Jonathan Scarlett, editors, *International Conference on Machine Learning, ICML 2023, 23-29 July 2023, Honolulu, Hawaii, USA*, volume 202 of *Proceedings of Machine Learning Research*, pages 38087–38099. PMLR, 2023.

[Yin *et al.*, 2023] Zhangyue Yin, Qiushi Sun, Qipeng Guo, Jiawen Wu, Xipeng Qiu, and Xuanjing Huang. Do large language models know what they don’t know? In Anna Rogers, Jordan L. Boyd-Graber, and Naoaki Okazaki, editors, *Findings of the Association for Computational Linguistics: ACL 2023, Toronto, Canada, July 9-14, 2023*, pages 8653–8665. Association for Computational Linguistics, 2023.

[Zellers *et al.*, 2019] Rowan Zellers, Ari Holtzman, Yonatan Bisk, Ali Farhadi, and Yejin Choi. Hellaswag: Can a machine really finish your sentence? In *Proceedings of the 57th Annual Meeting of the Association for Computational Linguistics*, 2019.

[Zhan *et al.*, 2025] Zaifu Zhan, Shuang Zhou, Min Zeng, Kai Yu, Meijia Song, Xiaoyi Chen, Jun Wang, Yu Hou, and Rui Zhang. Quantized large language models in biomedical natural language processing: Evaluation and recommendation. *CoRR*, abs/2509.04534, 2025.

[Ziyu *et al.*, 2023] Zhuang Ziyu, Chen Qiguang, Ma Longxuan, Li Mingda, Han Yi, Qian Yushan, Bai Haopeng, Zhang Weinan, and Ting Liu. Through the lens of core competency: Survey on evaluation of large language models. In *Proceedings of the 22nd Chinese National Conference on Computational Linguistics (Volume 2: Frontier Forum)*, pages 88–109, 2023.

A Appendix for “LLMs vs. Their Quantized Variants: Benchmarking the Illusion of Equivalence”

In the appendix, we give implementation-level details of legacy and K-quantization, and provide the full set of layer-wise statistics, divergence plots, and the complete performance tables that complement the main results.

A.1 Background

Quantization is a compression technique that reduces the precision of neural network weights from floating-point values to lower-bit integer to reduce model size, memory bandwidth demands, and faster and more efficient inference on resource-constrained hardware. We focus on two quantization methods: Legacy Quantization and K-Quantization[Lee, 2025].

A.2 Legacy Quantization

Legacy quantization in `llama.cpp` refers to the original low-bit quantization schemes, including Q8_0, Q5_0, and Q4_0, implemented within the `ggml` backend. Legacy schemes are categorized into two types: Type 0 (symmetric) and Type 1 (asymmetric) quantization. In this work, we focus on Type 0, which employs block-wise symmetric uniform quantization, converting contiguous groups of 32-bit floating-point weights into integer representations with 8, 5, or 4-bit precision.

The quantization is applied independently to each block of weights in three steps:

1. **Block Partitioning:** The input weight vector $\mathbf{x} \in \mathbb{R}^N$ is divided into fixed-size blocks of length q_k .
2. **Dynamic Range Determination:** For each block, the maximum absolute value is computed as in Eq. (2), which defines the dynamic range of the block and serves as the basis for scale computation: $a_{\max} = \max_i |x_i|$.
3. **Scale Computation:** A block-specific scaling factor d is derived by mapping the continuous weight range to the signed integer range determined by the bit-width b as computed in Eq. (3). The reciprocal $1/d$ is used to normalize weights prior to integer conversion. For example, Q4_0 ($b = 4$) uses quantization levels in $[-8, 7]$, whereas Q8_0 ($b = 8$) uses $[-128, 127]$.

$$d = \frac{a_{\max}}{2^{b-1} - 1}, \quad (3)$$

4. **Weight Quantization and Packing:** Each normalized weight is rounded to the nearest integer and saturated to the representable range as computed in Eq. (4). The resulting integers are stored using format-specific packing strategies. In Q4_0, two 4-bit signed values are packed into a single byte. For Q5_0, the four lower bits of each value are stored directly, while the most significant bit of each quantized weight is stored separately in a bit-mask array (`qh`). In Q8_0, each quantized value is stored as a signed 8-bit integer. To preserve resolution with minimal overhead, the scale factor d is stored in half-precision (FP16).

$$q_i = \text{clamp}\left(\text{round}\left(\frac{x_i}{d}\right), -2^{b-1}, 2^{b-1} - 1\right). \quad (4)$$

5. **Dequantization (Inference):** During inference, floating-point weights are reconstructed as computed as $\hat{x}_i = d \cdot q_i$.

The legacy quantization methods in `llama.cpp`, specifically `Q4_0`, `Q5_0`, and `Q8_0`, represent early efforts to balance model compactness and inference efficiency on CPU and consumer-grade GPU hardware. These schemes are simple, deterministic, hardware-agnostic, and do not require calibration or retraining.

A.3 K-Quantization

K-Quantization extends legacy quantization techniques by introducing more advanced scaling, min-deduction, and block-based encoding schemes for low-bit representations. These methods enable finer-grained adaptation to weight distribution heterogeneity, improving accuracy for sensitive layers. The process can be summarized as a deterministic 7-step procedure applied independently to each block of weights.

1. **Block Division:** The input weight row $\mathbf{x} \in \mathbb{R}^k$ is divided into Continuous blocks of size QK_K .
2. **Compute Local Scales and Minimums:** For each sub-block (e.g., 16 or 32 elements depending on the target bit-width), the local minimum x_{\min} and maximum x_{\max} are computed as $x_{\min} = \min_i x_i$, $x_{\max} = \max_i x_i$, defining the local input range. The initial scale s is estimated as $s = \{x_{\max} - x_{\min}\} / n_{\max}$, where n_{\max} is the maximum integer representable for the chosen bit-width. Optionally, s and x_{\min} are refined via a weighted least-squares approach to minimize quantization error. The maximum scale and minimum within the block are tracked for subsequent normalization.
3. **Normalize Scales:** The inverse scale factors are computed to map local scales to the target bit-width. The scale values are then quantized by nearest-integer rounding $\tilde{s} = \text{round}\left(\frac{1}{s}\right)$, ensuring consistent resolution across blocks.
4. **Encode Quantized Values:** Each element in the block is normalized by its corresponding scale factor and, if applicable, adjusted by the block minimum:

$$q_i = \text{clamp}\left(\text{round}\left(\frac{x_i - x_{\min}}{s}\right), 0, n_{\max}\right), \quad (5)$$

where $\text{clamp}(\cdot)$ ensures the quantized values remain within the valid integer range.

5. **Bit Packing:** Quantized values are efficiently packed into byte arrays. For higher bit-width formats (e.g., `Q5_K`, `Q6_K`), extra high bits are stored separately in auxiliary arrays. Per-block scale and minimum values are stored in compressed form (typically FP16) to preserve resolution with minimal overhead.
6. **Dequantization:** During inference, the original weights are reconstructed by multiplying the stored quantized integers by their corresponding scales and adding back the minimum offset if applicable:

$$\hat{x}_i = s \cdot q_i + x_{\min}, \quad (6)$$

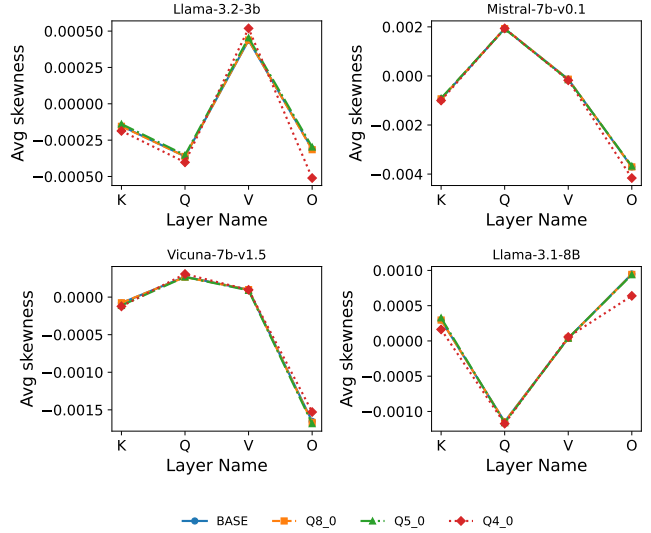


Figure 6: Average skewness Legacy Quant.

using auxiliary high-bit masks when necessary for higher bit-width formats.

7. **Weighted Variants:** Some implementations allow per-element weights to bias the quantization process, improving fidelity for elements with higher variance. Weighted quantization follows the same procedure as above but incorporates the per-element weight into the least-squares scale refinement.

A.4 Statistical Changes in Attention Layers

For each block i , we compute a block-level metric by averaging $s(W_i^Q)$, $s(W_i^K)$, $s(W_i^V)$, and $s(W_i^O)$, and then average these values across all N blocks as in Eq. (1). The results are shown in Figure 1.

In Figure 1, higher-bit quantization (8 to 5 bits) consistently preserves stable distribution statistics, maintaining near-zero mean, low skewness, stable kurtosis, and base level standard deviation across models. In contrast, aggressive quantization to (4 to 2) bits, particularly `Q3_K` and `Q2_K`, introduces distortions characterized by increased skewness and variance, reduced kurtosis, and systematic mean shifts, with model-specific sensitivity (e.g., larger deviations in `Llama-3.2-3B`). Notably, `Q5_K` often matches or improves upon base behavior, indicating superior preservation of distributional integrity.

Individual Statistic Comparison We compute the average value of each statistical measure for every type of attention layer across all N blocks as shown in Eq. (2). Then, We build figures showing the differences between quantization levels. The figures show the average statics metrics across the Key (K), Query (Q), Value (V), and Output (O) layers for the four LLMs.

In all four models, the average stat curves(skewness, kurtosis, mean, and STD) of legacy quantization for all four quantization levels are almost overlaid. This consistency indicates that these Legacy quantization schemes are highly ef-

fective at preserving the original model’s average stats properties. For example, figure 6 illustrates the average skewness of the **K**, **Q**, **V**, and **O** (output) attention layer weights across different legacy quantization levels (Q8_0, Q5_0, Q4_0) compared to the Base model. For all four LLMs, the legacy quantization methods do not significantly alter the average skewness of the individual attention layers; the Q8_0, Q5_0, and Q4_0 lines closely overlap the baseline.

The results also show that moderate K-quantization (Q6_K–Q4_K) effectively preserves attention-layer statistics across **Q**, **K**, **V**, and **O**, maintaining near-zero skewness and mean, kurtosis, and standard deviation, which demonstrates stable distribution shape, tail behavior, and variance control. In contrast, aggressive Q3_K and Q2_K introduce large distortions—volatile skewness and mean, reduced kurtosis, and slightly lower standard deviation, particularly in **Q** and **K**, indicating breakdown of statistical stability at extreme compression, while **V** and **O** preserve their relative statistical characteristics. Figures 2 and 3 illustrate the skewness and kurtosis behavior, respectively.

Analysis of skewness, kurtosis, mean, and standard deviation shows that Legacy quantization (Q8_0, Q5_0, Q4_0) has minimal impact, with curves nearly identical to base across all layers. Moderate K-quantization (Q6_K–Q4_K) similarly preserves distributions, while aggressive Q3_K and Q2_K introduce substantial distortions—especially in **K** and **Q** layers—making statistics volatile or flattened.

A.5 Distributional Divergence in Attention Layers

Subsequently, we calculate the average divergence across blocks and block-wise divergence as described in Section 3.2.

Average Divergence Across All Attention Layers: We compute the average value of each divergence measure, from the base to each quantized variant, for each type of attention layer across all N blocks.

Figure 4 illustrates different aspects of quantization’s effect on four distinct LLMs across various quantization levels, from Q8_0 to Q2_K. The average cosine similarity shows moderate sensitivity, remaining high in the less aggressive quantization levels (Q8_0 to Q5_K), but then exhibiting a significant drop for all models at the lowest Q2_K level, with Vicuna-7B maintaining the best angular relationship (highest cosine) across the board. The average Euclidean distance remains relatively constant across all quantization levels, with Vicuna-7B exhibiting a consistently high magnitude separation (≈ 70) while Mistral-7B shows the lowest (≈ 10). Finally, the **average KL divergence** and **average KS statistic** demonstrate extremely high sensitivity to the quantization level, peaking sharply at Q3_K and Q4_0 respectively, and bottoming out at Q8_0, Q5_K and Q4_K where the distributions are minimally altered.

Individual Divergence Comparison: We compute the average value of each divergence measure for every type of attention layer in all N blocks. as shown in Eq. (2).

The results show that legacy quantization consistently preserves **V** and **O** weights, with high cosine similarity and low Euclidean distance, while **K** and **Q** layers are largely altered. KL divergence analyses further reveal that **K** and

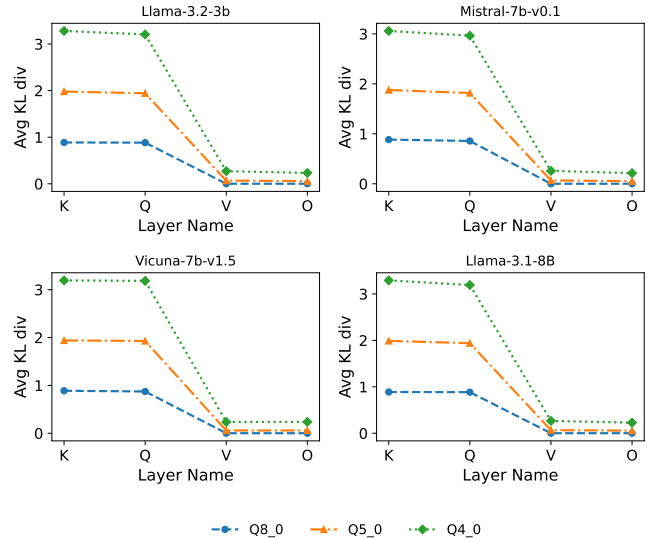


Figure 7: Average KL Legacy Quant.

Q are the most statistically sensitive, exhibiting the highest divergence—especially at Q4_0—and that distributional shifts increase with quantization aggressiveness. Overall, Legacy schemes primarily distort the statistical structure of **K** and **Q** layers while leaving **V** and **O** largely unaffected. Figures 7 and 8 illustrate the KL and KS behavior, respectively.

The results show that legacy quantization consistently preserves **V** and **O** weights, with high cosine similarity and low Euclidean distance, while **K** and **Q** layers are largely altered.

The results show that under K-quantization, **V** and **O** layers are largely preserved, with high cosine similarity, near-zero Euclidean distance, and low KL divergence, while **K** and **Q** layers undergo greater changes. These layers exhibit the highest KL divergence, particularly at Q3_K and Q2_K, indicating that K-quantization primarily alters their statistical distributions in a bit-width-dependent manner, reflecting their higher sensitivity to compression. Figures 5 and 9 illustrate the KL and KS behavior, respectively.

A.6 Performance Evaluations

We evaluate the models on C4 [Raffel *et al.*, 2020] and WikiText-2 [Merity *et al.*, 2017] to measure perplexity. Table 2 and 3 show that Q3_K consistently delivers the strongest quantization results, achieving the lowest perplexity across most models. Notably, Llama-3.2-3B and Vicuna-7B both show Q3_K outperforming other configurations, including the Base model, demonstrating its ability to preserve expressiveness while providing significant compression.

Q5_K consistently maintains perplexity extremely close to or sometimes better than the base model on both C4 and WikiText-2. In Llama-3.2-3B and Vicuna-7B, Q5_K achieves some of the strongest C4 results, and across all models it avoids the sharp performance drops seen in more aggressive quantization levels. This makes Q5_K a good choice when prioritizing robustness alongside compression efficiency. Mistral-7B and Llama-3.1-8B exhibit different behaviors, with each model responding uniquely to

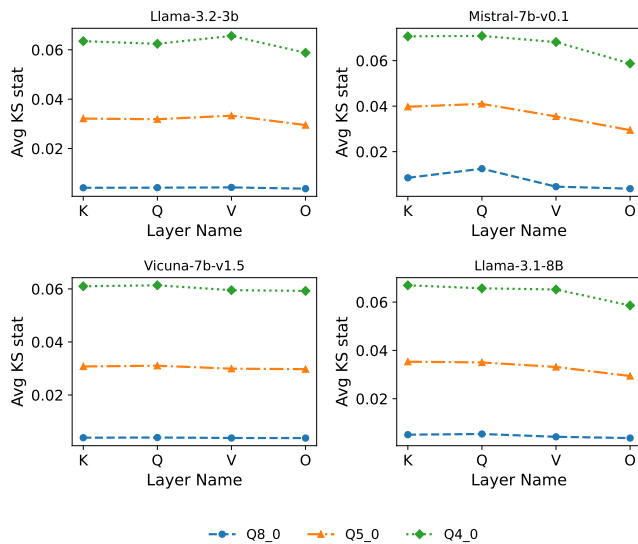


Figure 8: Average KS Legacy Quant.

quantization. Mistral-7B is highly resilient, showing minimal degradation across quantization levels; its best C4 performance appears at Q6_K, although Q3_K and Q5_K remain strong and stable. In contrast, Llama-3.1-8B shows greater sensitivity: aggressive quantization such as Q2_K and Q3_K reduces perplexity on WikiText-2 but degrades performance on C4, revealing dataset-dependent instability. For Llama-3.1-8B, the most balanced choice is Q5_K, which preserves near-Base performance on both datasets while avoiding the volatility of more extreme quantization settings.

In addition, we evaluated the models on zero-shot benchmarks to assess their generalization capabilities across various domains. These datasets, each with unique characteristics, include **HellaSwag** [Zellers *et al.*, 2019], **Winogrande** [Sakaguchi *et al.*, 2019], and **ARC** (AI2 Reasoning Challenge) [Clark *et al.*, 2018]. These are benchmark datasets designed to evaluate commonsense reasoning and multi-step problem-solving in language models. They test a model’s ability to complete narratives, resolve ambiguous pronouns, and answer grade-school science questions, respectively. We use accuracy and Correctness Agreement to evaluate the models. Correctness Agreement assess the behavioral consistency between the base model and its quantized variants. This metric uses the correctness label (Correct/Incorrect) as the binary output for the Hamming comparison. It provides a direct and interpretable measure of alignment between the decision behaviors of the two models, independent of their absolute accuracy values.

Table ?? shows the average accuracy of HellaSwag, Winogrande, and ARC across all models and their quantized variants. The Base variants consistently achieve the highest accuracy, with a clear drop once quantization is applied. Mistral-7B maintains the strongest overall performance and shows the most stable accuracy across quantization levels, while Llama-3.2-3B experiences the strongest decline, especially at Q2_K. Vicuna-7B

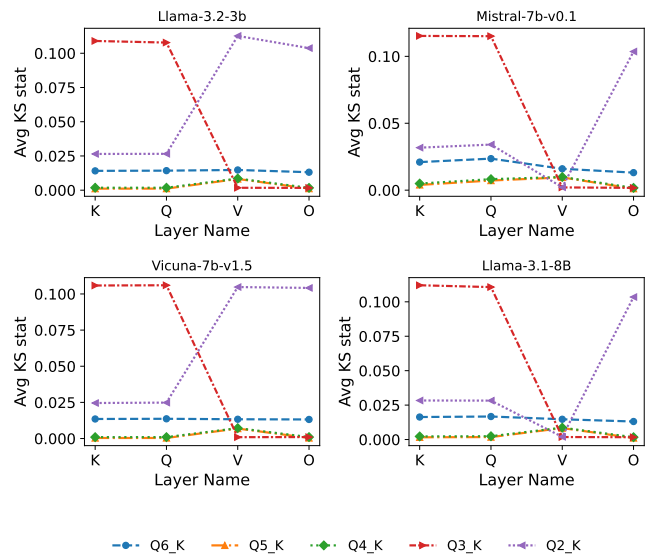


Figure 9: Average KS K-Quantization.

and Llama-3.1-8B show moderate degradation, with occasional small recoveries around mid-range quantization (Q5_K–Q4_K). Overall, accuracy generally decreases as quantization becomes more aggressive, and lower-bit variants consistently under-perform higher-bit ones.

Table ?? shows the average agreement of HellaSwag, Winogrande, and ARC between all models and their quantized variants. Llama-3.2-3B shows the largest spread, with agreement gradually decreasing from Q8_0 through Q4_K and then dropping sharply at Q3_K and Q2_K—indicating that lower-bit quantization significantly harms consistency for this smaller model. Vicuna-7B fluctuates between Q8_0 and Q3_K, but it experiences a pronounced drop at Q2_K, suggesting that only ultra-low-bit quantization substantially impacts it. Mistral-7B is the most robust within-model: its agreement varies by less than one point across all quantization levels, and even Q2_K retains strong performance, showing that the model handles compression exceptionally well. Llama-3.1-8B shows moderate variation: it stays tightly clustered from Q8_0 to Q4_K but dips at Q5_K and drops more noticeably at Q2_K, reflecting moderate sensitivity compared to the other 7B models but still more resilience than the 3B model.